

# Attentional Multilabel Learning over Graphs

## A message passing approach

Kien Do · Truyen Tran · Thin Nguyen ·  
Svetha Venkatesh

Received: date / Accepted: date

**Abstract** We address a largely open problem of multilabel classification over graphs. Unlike traditional vector input, graph has rich variable-size structures, that suggests complex relationships between labels and subgraphs. Uncovering these relations might hold the keys of classification performance and explainability. To this end, we design GAML (**G**raph **A**ttentional **M**ulti-**L**abel learning), a graph neural network that models the relations present in the input graph, in the label set, and across graph-labels by leveraging the message passing algorithm and attention mechanism. Representation of labels and input nodes is refined iteratively through multiple steps, during which interesting subgraph-label patterns emerge. In addition, GAML is highly flexible by allowing explicit label dependencies to be incorporated easily. It also scales linearly with the number of labels and graph size thanks to our proposed *hierarchical attention*. These properties open a wide range of applications seen in the real-world. We evaluate GAML on an extensive set of experiments with both graph inputs (for predicting drug-protein binding, and drug-cancer response), and classical unstructured inputs. The results are significantly better than well-known multilabel learning techniques.

**Keywords** Multilabel learning · Graph classification · Graph neural networks · Message passing

---

This work is partially supported by the Telstra-Deakin Centre of Excellence in Big Data and Machine Learning.

---

Kien Do, Truyen Tran, Thin Nguyen and Svetha Venkatesh  
Applied AI Institute, Deakin University, Australia  
E-mail: {dkdo, truyen.tran, thin.nguyen, svetha.venkatesh}@deakin.ed.au

## 1 Introduction

Drug development costs billions of dollars over many years with multiple stages of refinement and trial [27]. For this reason, repurposing approved drugs is considered as a critical alternative to the full development cycle, which offers a huge saving of money, time, and lives. The goal of repurposing is to predict the drug effect on multiple related diseases. This can naturally be formulated as a multilabel learning problem. However, different from standard domains like text or image, drugs are usually represented as variable size graphs of atoms linked by chemical bonds. The irregularity and complexity of rich graph structures make multilabel learning over molecular graph very challenging. Therefore, a proper way of treatment is demanded.

We hypothesize that the key for classification performance and explainability lies in uncovering the relationships between labels and molecular subgraphs. Towards this goal, we design a new variant of graph neural network [34] called GAML (which stands for **G**raph **A**ttentional **M**ulti-**L**abel learning). GAML treat all classes as nodes (termed label nodes) and merge them with other nodes (called input nodes) in the input graph to form an unified label-input graph. In the joint graph, correlations between labels and substructures can be effectively captured through the interaction across the label nodes and the input nodes. Specifically, we leverage the message passing algorithm [30,35,14] to simultaneously update the local substructure at every input node and to propagate the substructure-contained messages from all the input nodes to the label nodes. By using attention [2,49], each label node can extract the most related substructures to update its own state which will later be used to predict the present of the corresponding class. Attention also enables insightful visualization which helps explain the prediction. To account for large number of classes and big input graph, we propose a new type of attention named *hierarchical attention*. Different from the standard approach that calculates the score matrix between every input and label node directly, our attention mechanism uses some intermediate *attentional factors* to save computation. In our model, implicit dependencies among the labels are captured via common attended substructures. However, when the explicit dependencies among the labels are available (e.g, through expert knowledge), GAML can easily integrate them by adding links and exchange messages between the associated label nodes. Moreover, since the node update procedure run iteratively, our model can learn the label-subgraph correlation at various resolution scales of structures.

The flexibility and scalability of GAML open up a wide range of applications seen in the real-world. In this paper, we focus on two major drug-multi-target prediction problems: predicting *drug-protein binding*, and *drug-cancer response*. We also test our method on classical unstructured input, which is a degenerating case of graph. In all cases, GAML proves to be superior against rival multilabel learning techniques.

In summary, our contributions are:

- Addressing a largely open problem of multilabeling over graphs. We propose a novel and scalable neural graph network that explicitly models the (multi-

way) relationship among labels and graph data. The network permits label descriptors (and embedding), as well as label dependency prior.

- An extensive suit of experiments to demonstrate the advantages of our method in two settings: graph-structured input and unstructured input.

## 2 Related Work

*Multilabel classification with label dependency* Multilabel learning has attracted a great deal of research in machine learning. Most work focuses on capturing the implicit or explicit label dependencies. One strategy is applying Canonical Correlation Analysis (CCA) to map input and label into a common latent space. Then from this space, the model will reconstruct the target label. Extensions of this approach including both shallow [39, 24] and deep [50] models. For graphical model-based approach, [13] uses Conditional Random Fields to model the three way relationship between every pair of labels  $i, j$  and the input  $\mathbf{x}$  using a feature function  $\phi(y_i, y_j, \mathbf{x})$ . Meanwhile, [17] constructs a fully connected cyclic Bayesian Network over labels and perform structure learning on this network. The probability of a label  $y_i$  conditioned on the input  $\mathbf{x}$  and other labels  $y_{-i}$  is modeled using a logistic regression network. Both methods are computationally expensive and require inexact inference for large number of labels.

To model the joint distribution of labels but still keep computation reasonable, some methods exploit chain rule factorization. The most notable one is Probabilistic Classifier Chain [9] which builds a separate binary classifier for each label with input to the model is the combination of the original input and the predicted labels. Other methods follow that idea but use recurrent neural networks [47, 6] to learn the correlations better. However, the critical issues of these method are *ordering* and *poor inference* (since the the output label at one step depends on the value of the previous predicted labels not their distribution, which is very unstable). Although some tricks like beam search [47], or automatic order selection [6] are implemented to improve the results, they can only solve part of the problems.

Expert knowledge about label dependencies represented as trees [10] or graphs [3, 5] has been exploited for multilabel/multiclass classification. In [5], the authors build a graph neural network over the predefined label graph. The input vector is copied for every label node and is concatenated to the label embedding vector to form an initial state for that label node. Their method, however, is limited to the vector input only whereas our model directly works on graph input with vector input is the special case.

*Multilabel classification with graph inputs* Although graph classification has attracted a significant interest in recent years [40], there has been a limited body of work on multilabel graph classification [22]. The line of work on image tagging considers multilabel learning over a grid of pixels [15, 48, 47]. However, the standard treatment using CNN usually focus on attention over feature maps instead of exploiting the relationship structure of objects in the original

image. A recent work in visual question answering that push forward this idea is [41], but the QA setting is different from ours. A special case of our multilabel learning over graphs is multilabel learning over set[31] where input is a collection of nodes with no explicit links.

*Graph neural networks* By leveraging the representation power of deep neural networks such as CNN and RNN, a wide range of methods for learning over graphs [34, 25, 28, 8, 21, 30, 18, 14] has been proposed recently. These methods can be grouped into more general categories such as Spectral Graph based [4, 8, 21], Message Passing based [30, 35, 14], Random Walk based [29, 16], Neural Net based [25]. Among them, Message Passing Graph Neural Networks (MPGNNs) are very powerful since they can handle various kinds of graphs including molecular graphs where edges and nodes both have types. MPGNNs have found many applications in bioinformatics such as drug activity classification [32], chemical properties prediction [14], protein interface prediction [11] and drug generation [19]. However, none of these methods properly handle multilabel classification problems in which modeling multi-way relationships among labels and molecular subgraphs is the key factor.

### 3 Method

In this section, we present our main contribution—the GAML (Graph Attentional Multi-Label learning). First we provide background knowledge about graph neural networks, on which GAML is built.

#### 3.1 Preliminaries: Message passing graph neural network

Consider an attributed graph  $\mathcal{G} = (\mathcal{V}, \mathcal{E})$  where  $\mathcal{V}$  is the set of nodes and  $\mathcal{E}$  is the set of edges. Each node  $i$  is associated with a feature vector  $\mathbf{v}_i$  and each edge  $(i, j)$  is associated with an attribute set  $\mathbf{e}_{ij}$  (e.g. weight, type, features). In case node  $i$  has type  $t_i$ ,  $\mathbf{v}_i$  can be an embedding vector of  $t_i$ . Let  $\mathbf{x}_i$  be a state of node  $i$  and  $\mathcal{N}(i) = \{j \mid (i, j) \in \mathcal{E}\}$  denote the neighborhood of node  $i$ . In message passing graph neural networks [34, 30, 14], a node uses information from its neighbors to update its own state:

$$\mathbf{x}_i^t \leftarrow f\left(\mathbf{x}_i^{t-1}, \{(\mathbf{x}_j^{t-1}, \mathbf{e}_{ij})\}_{j \in \mathcal{N}(i)}\right) \quad (1)$$

where  $t$  denotes update step; and  $f(\cdot)$  is a non-linear function (e.g., a multilayer perceptron (MLP)). At  $t = 0$ , we set  $\mathbf{x}_i^0 = \mathbf{v}_i$ .

Eq. (1) is generic for most graph neural network models. In practice, it can be divided into two steps: *message aggregation* and *state update*. In the *message aggregation* step, we combine multiple messages sent to node  $i$  into a single message vector  $\mathbf{m}_i$ :

$$\mathbf{m}_i^t = g^a\left(\mathbf{x}_i^{t-1}, \{(\mathbf{x}_j^{t-1}, \mathbf{e}_{ij})\}_{j \in \mathcal{N}(i)}\right) \quad (2)$$

where  $g^a(\cdot)$  can be an attention [2, 49] or a pooling architecture. For example, the message aggregated using mean pooling has the following formula:

$$\mathbf{m}_i^t = \frac{1}{|\mathcal{N}(i)|} \sum_{j \in \mathcal{N}(i)} W_{e_{ij}} \mathbf{x}_j^{t-1} \quad (3)$$

for some parameter matrix  $W_{e_{ij}}$ . Despite of simplicity, Eq. (3) has shown to be able to encode graph structures in several message passing models [30, 35, 14].

During the *state update* step, the node state is updated as follows:

$$\mathbf{x}_i^t \leftarrow g^u(\mathbf{x}_i^{t-1}, \mathbf{m}_i^t) \quad (4)$$

where  $g^u(\cdot)$  can be any type of deep neural networks such as MLP [21, 18], RNN [34], GRU [25] or Highway Net [30]. In our model, we use Highway Net [38] for  $g^u(\cdot)$  as it has shown to be effective for long range dependencies thanks to its skip-connection and gating mechanism. As a result, Eq. (4) now becomes:

$$\mathbf{x}_i^t \leftarrow (1 - \boldsymbol{\alpha}_i^t) \odot \mathbf{x}_i^{t-1} + \boldsymbol{\alpha}_i^t \odot \hat{\mathbf{x}}_i^t \quad (5)$$

where  $\boldsymbol{\alpha}_i^t$  and  $\hat{\mathbf{x}}_i^t$  are the gate vector and the non-linear candidate vector of node  $i$  at time  $t$ , respectively;  $\odot$  is the element-wise product. The formulas of  $\boldsymbol{\alpha}_i^t$  and  $\hat{\mathbf{x}}_i^t$  are provided below:

$$\begin{aligned} \boldsymbol{\alpha}_i^t &= \text{sigmoid}(W_\alpha \mathbf{x}_i^{t-1} + U_\alpha \mathbf{m}_i^t + \mathbf{b}_\alpha) \\ \hat{\mathbf{x}}_i^t &= \text{relu}(W_x \mathbf{x}_i^{t-1} + U_x \mathbf{m}_i^t + \mathbf{b}_x) \end{aligned}$$

where  $W_\alpha, W_x, U_\alpha, U_x$ , and  $\mathbf{b}_\alpha, \mathbf{b}_x$  are parameters which can be different or shared among layers. During experiments, we observed that models with parameter sharing run faster but still provide comparable results. Hence, we applied this sharing scheme to our model.

After  $T$  steps of message passing,  $\mathbf{x}_i^T$  would capture the graph substructure around node  $i$  up to  $T$  hops. The graph summary vector  $\mathbf{x}_G$  is the combination of the state vector of all nodes in the graph at step  $T$ . In the simplest form,  $\mathbf{x}_G$  is the average of  $\{\mathbf{x}_i^T\}_{i \in \mathcal{V}}$ , as follows:

$$\mathbf{x}_G = \frac{1}{|\mathcal{V}|} \sum_{i \in \mathcal{V}} \mathbf{x}_i^T$$

### 3.2 Multilabel learning over graphs

Multilabel graph classification associates a graph  $\mathcal{G}$  with a label vector  $\mathbf{y} = (y_1, \dots, y_C) \in \{0, 1\}^C$  where  $y_c = 1$  indicates that class  $c$  presents conditioned on  $\mathcal{G}$ . We argue that in order to perform well on this task, two correlation structures must be captured: those *within the label set* and those *between the label set and input subgraphs*.

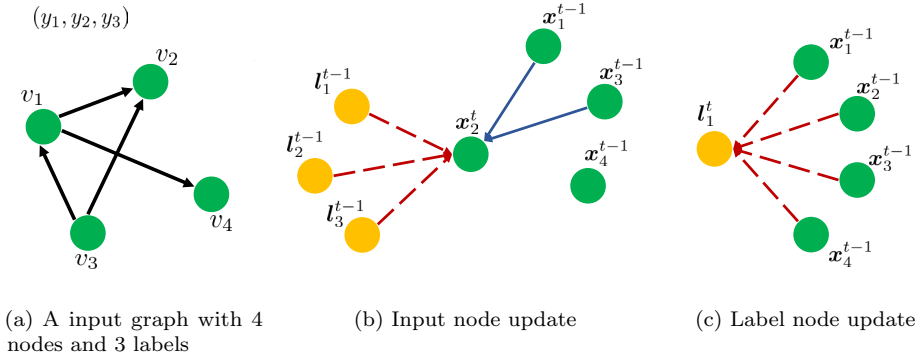


Fig. 1: Message passing in the joint graph of input nodes and label nodes. In (b) and (c), dash red link indicates message passing with attention while blue solid link indicates message passing with mean pooling

Let us start with representing labels in the same vector space. When prior label descriptors exist, the space is simply the descriptor vector space. Otherwise, labels are embedded using a *class embedding matrix*  $M \in \mathbb{R}^{C \times d_l}$  as follows:

$$\mathbf{l}_c^0 = M \mathbf{1}_c$$

where  $\mathbf{1}_c \in \mathbb{R}^C$  is an one-hot vector with the  $c$ -th element equal to 1.

For an input graph  $\mathcal{G}$ , we then consider all the  $C$  classes as auxiliary nodes (called *label nodes*) alongside  $|\mathcal{V}|$  existing nodes of the input graph  $\mathcal{G}$ . Each label node  $c$  has the initial state  $\mathbf{l}_c^0$  and connects to all input nodes. Similarly, each input node  $i$  also connects to all label nodes. It results in a joint graph of  $C + |\mathcal{V}|$  nodes, which naturally lend itself to the message passing scheme in the graph neural network presented in Section 3.1. The idea is that by iteratively updating the states of input and label nodes using message passing, complex label-label and label-substructure dependencies emerge. See Fig. 1 for an illustration.

### 3.2.1 Input node update

Since an input node  $i$  connects to its neighbor nodes  $j \in \mathcal{N}(i)$  and all the class node  $c \in \overline{1, C}$ , the message passing update of the input node  $i$  at step  $t$  is formulated as follows:

$$\mathbf{x}_i^t = f\left(\mathbf{x}_i^{t-1}, \left\{(\mathbf{x}_j^{t-1}, \mathbf{e}_{ij})\right\}_{j \in \mathcal{N}(i)}, \left\{\mathbf{l}_c^{t-1}\right\}_{c \in \overline{1, C}}\right) \quad (6)$$

Note that Eq. (6) is derived from Eq. (1) with the introduction of new arguments  $\left\{\mathbf{l}_c^{t-1}\right\}_{c \in \overline{1, C}}$ .

There are two types of message sent to the input node  $i$ . One contains structure information from neighbor input nodes and the other contains label-related information from label nodes. Because these messages have different meanings, they should be aggregated into separate message vectors. In case of neighbor input nodes, we use mean pooling as similar to Eq. (3):

$$\boldsymbol{\mu}_i^t = \frac{1}{|\mathcal{N}(i)|} \sum_{j \in \mathcal{N}(i)} W_{e_{ij}} \mathbf{x}_j^{t-1}$$

However, mean pooling is not ideal to aggregate labels since it equalizes the importance of each class towards the input node  $i$ . To overcome this issue, we use the attention mechanism [2, 49] to compute a weighted sum of all the label nodes as follows:

$$\mathbf{m}_i^t = \sum_{c=1}^C a_{ic}^t \mathbf{l}_c^{t-1} \quad (7)$$

where  $a_{ic}^t \in \mathbb{R}$  is the attention coefficient from the input node  $i$  to a label node  $c$  at time  $t$ , computed as:

$$s_{ic}^t = \mathbf{u}_s^\top \tanh(W_s \mathbf{x}_i^{t-1} + U_s \mathbf{l}_c^{t-1} + \mathbf{b}_s) \quad (8)$$

$$a_{ic}^t = \frac{\exp(s_{ic}^t)}{\sum_{c'=1}^C \exp(s_{ic'}^t)} \quad (9)$$

The set of all unnormalized attention scores  $s_{ic}^t$  in Eq. (8) forms a matrix  $S^t \in \mathbb{R}^{|\mathcal{V}| \times C}$ , which we will reuse later.

For generality, Eqs. (7–9) are written in a more compact form:

$$\mathbf{m}_i^t = \text{Attention} \left( \mathbf{x}_i^{t-1}, \{ \mathbf{l}_c^{t-1} \}_{c \in \overline{1, C}} \right) \quad (10)$$

We call the attention in Eq. (10) *input-to-label* attention.

In the state update phase, the new state  $\mathbf{x}_i^t$  of the input node  $i$  is computed as:

$$\mathbf{x}_i^t = \text{Highway} \left( \mathbf{x}_i^{t-1}, [\boldsymbol{\mu}_i^t, \mathbf{m}_i^t] \right)$$

where  $[\cdot]$  denotes vector concatenation.

### 3.2.2 Label node update

By connecting to every input node, a label node  $c$  can receive information about various substructures in the graph  $\mathcal{G}$  through multiple steps of message passing. Among these substructures, a few may be related to the class  $c$ . Therefore, we use the attention mechanism to extract the most useful substructures for predicting class  $c$  and store them in the message vector as follows:

$$\mathbf{m}_c^t = \text{Attention} \left( \mathbf{l}_c^{t-1}, \{\mathbf{x}_i^{t-1}\}_{i \in \overline{1, |\mathcal{V}|}} \right) \quad (11)$$

where  $\text{Attention}(\cdot)$  is similar to the function defined in Eq. (10) with the role of input nodes and label nodes swapped. We denote this function *label-to-input* attention. The unnormalized score matrix  $S^t$  from Eq. (8) is reused here to save computation and improve consistency. However, the attention coefficients are normalized over rows instead of columns of  $S^t$ , i.e.,

$$a_{ci}^t = \frac{\exp(s_{ic}^t)}{\sum_{i=1}^{|\mathcal{V}|} \exp(s_{ic}^t)}$$

Finally, we compute the new state of the label node  $c$  using Highway Net as:

$$\mathbf{l}_c^t = \text{Highway}(\mathbf{l}_c^{t-1}, \mathbf{m}_c^t)$$

### 3.2.3 A priori label dependency

When explicit label dependency is available, a label graph can be formed in the same way as the input graph. Messages between label nodes is aggregated using mean-pooling as in Eq. (3):

$$\boldsymbol{\mu}_c^t = \frac{1}{|\mathcal{N}(c)|} \sum_{f \in \mathcal{N}(c)} W_{ef} \mathbf{l}_f^{t-1}$$

The state of the label node  $c$  is updated as:

$$\mathbf{l}_c^t = \text{Highway}(\mathbf{l}_c^{t-1}, [\mathbf{m}_c^t, \boldsymbol{\mu}_c^t])$$

### 3.2.4 Vector input as a special case

In many traditional multilabel classification problems, the input is represented as vector instead of graph. This can be seen as a special case of our model where the input graph  $\mathcal{G}$  collapses into a single node  $\mathbf{x}$ . With this observation, the state update of the input node at step  $t$  is:

$$\begin{aligned} \mathbf{m}^t &= \text{Attention} \left( \mathbf{x}^{t-1}, \{\mathbf{l}_c^{t-1}\}_{c \in \overline{1, C}} \right) \\ \mathbf{x}^t &= \text{Highway}(\mathbf{x}^{t-1}, \mathbf{m}^t) \end{aligned}$$



The state of label node  $c$  is updated as:

$$\mathbf{l}_c^t = \text{Highway}(\mathbf{l}^{t-1}, \mathbf{x}^{t-1})$$

### 3.2.5 Learning

After  $T$  steps of message passing, we pass each class-specific final state vector  $\mathbf{l}_c^T$  to a shared multi-layer perceptron (MLP) with sigmoid activation on top to predict the present of class  $c$ :

$$o_c = \text{MLP}(\mathbf{l}_c^T)$$

Here the value of  $o_c$  is in  $(0, 1)$ . For learning, we use a binary cross-entropy loss function which is defined as:

$$\mathcal{L} = \mathbb{E}_{\text{train}} \left( \sum_{c=1}^C y_c \log o_c + (1 - y_c) \log(1 - o_c) \right)$$

where  $\mathbb{E}_{\text{train}}$  denotes the mean over all training data.

## 3.3 Scale to big graphs and many labels

When the number of nodes in the input graph ( $|\mathcal{V}|$ ) and the number of classes ( $C$ ) are large, it becomes expensive to calculate the unnormalized score matrix  $S^t \in \mathbb{R}^{|\mathcal{V}| \times C}$  in Eq. (8) for all steps  $t = 1, 2, \dots, T$ . To handle this problem, we propose a new attention technique called *hierarchical attention*. At each layer, we define  $K$  ( $K \ll \min\{|\mathcal{V}|, C\}$ ) intermediate *attentional factors* between input nodes and label nodes. The input-label attentions are broken down into two steps as follows:

- For *label-to-input* attention, we do *factor-to-input* attention then *label-to-factor* attention.
- For *input-to-label* attention, we do *factor-to-label* attention then *input-to-factor* attention.

*Label-to-input message aggregation.* More concretely, the *label-to-input* message aggregation in Eq. (7) is replaced by:

$$\mathbf{m}_i^t = \sum_{k=1}^K a_{ik}^t \boldsymbol{\lambda}_k^{t-1}; \quad \text{for} \quad \boldsymbol{\lambda}_k^{t-1} = \sum_{c=1}^C b_{ck}^t \mathbf{l}_c^{t-1}$$

where  $\boldsymbol{\lambda}_k^{t-1}$  is the  $k$ -th intermediate factor ( $k \in \overline{1, K}$ ) that aggregates all label nodes;  $\mathbf{m}_i^t$  is the message to the input node  $i$ ;  $a_{ik}^t$  is factor-to-input attention probability (i.e.,  $\sum_k a_{ik}^t$ ); and  $b_{ck}^t$  is label-to-factor attention probability (i.e.,  $\sum_c b_{ck}^t = 1$ ).

To compute  $a_{ik}^t$  and  $b_{ck}^t$  we define two score matrices  $S_1^t \in \mathbb{R}^{|\mathcal{V}| \times K}$  and  $S_2^t \in \mathbb{R}^{C \times K}$  as follows:

$$s_{1;ik}^t = \mathbf{u}_1^\top \tanh(W_1 \mathbf{x}_i^{t-1} + \mathbf{z}_k^{t-1}) \quad (12)$$

$$\text{and } s_{2;ck}^t = \mathbf{u}_2^\top \tanh(W_2 \mathbf{l}_c^{t-1} + \mathbf{z}_k^{t-1}) \quad (13)$$

where  $\mathbf{u}_1, \mathbf{u}_2 \in \mathbb{R}^{d_z}$ ,  $W_1 \in \mathbb{R}^{d_x \times d_z}$ ,  $W_2 \in \mathbb{R}^{d_l \times d_z}$  and  $\mathbf{z}_k^t \in \mathbb{R}^{d_z}$ , ( $k = \overline{1, K}$ ) are parameters. Then factor-to-input attention probability and label-to-factor attention probability are computed as:

$$a_{ik}^t = \frac{\exp(s_{1;ik}^t)}{\sum_{k'=1}^K \exp(s_{1;ik'}^t)}; \quad b_{ck}^t = \frac{\exp(s_{2;ck}^t)}{\sum_{c'=1}^C \exp(s_{2;c'k}^t)}$$

*Input-to-label message aggregation.* Likewise the two-step *input-to-label* message aggregation is computed as:

$$\mathbf{m}_c^t = \sum_{k=1}^K \alpha_{ck}^t \boldsymbol{\chi}_k^{t-1}; \quad \text{for } \boldsymbol{\chi}_k^{t-1} = \sum_{i=1}^{|\mathcal{V}|} \beta_{ik}^t \mathbf{x}_i^{t-1}$$

where  $\boldsymbol{\chi}_k^{t-1}$  is the  $k$ -th intermediate factor ( $k \in \overline{1, K}$ ) that aggregates all input nodes;  $\mathbf{m}_c^t$  is the message to the label node  $c$ ;  $\alpha_{ck}^t$  is factor-to-label attention probability (i.e.,  $\sum_k \alpha_{ck}^t = 1$ ); and  $\beta_{ik}^t$  is input-to-factor attention probability (i.e.,  $\sum_i \beta_{ik}^t = 1$ ). The attention probabilities are respectively computed as:

$$\alpha_{ik}^t = \frac{\exp(s_{1;ik}^t)}{\sum_{i'=1}^{|\mathcal{V}|} \exp(s_{1;i'k}^t)}; \quad \beta_{ck}^t = \frac{\exp(s_{2;ck}^t)}{\sum_{k'=1}^K \exp(s_{2;ck'}^t)}$$

where the scores  $s_{1;ik}^t$  and  $s_{2;ck}^t$  are computed using Eqs. (12,13).

It is clear that with this decomposition strategy, the number of computation steps reduces from  $\mathcal{O}(|\mathcal{V}|C)$  to  $\mathcal{O}((|\mathcal{V}| + C)K)$  for  $K \ll \min\{|\mathcal{V}|, C\}$ .

### 3.4 Detecting higher-order correlation

*Higher-order label correlation* The iterative message passing scheme spreads information to distant nodes. Two labels can indirectly interact with each other after two step of updates: a label sends messages to input nodes which then redistribute the information back to other labels. This brings about higher-order label correlation.

*Multi-resolution substructure-label correlation* Likewise, after  $t$  steps, an input node accumulates information from other nodes of  $t$  degrees of separation. In other words, the node state represents a subgraph of radius  $t$ . Thus, input-to-label attention detects substructures of the input graph with varying resolution.

## 4 Experiments

We present empirical results on two comprehensive sets of experiments: one on graph-structured input (Section 4.1) and the other on traditional unstructured input (Section 4.2).

### 4.1 Multilabel classification with graph-structured input

Our experiments focus on biochemical databases of potential drugs. A drug is a moderate-sized molecule with desirable bioactivities, which can be treated as labels. A molecular graph has nodes representing atoms and edges representing bond types.

#### 4.1.1 Datasets

We use two real-world biochemical datasets:

- *9cancers*: For this dataset, the goal is to predict drug activity against nine types of cancer (see Table. 1). The activity is binary indicating whether there is a response, i.e., the drug reduces or prevents tumor growth. We first download nine separate datasets for each cancer type from PubChem<sup>1</sup>. Then, we search for drug molecules that appear in all datasets, which results in about 22 thousand molecules in total. Among them, there are 3,356 molecules active for at least one type of cancer. We select all the active molecules and 10,000 fully inactive molecules to create the final dataset for experiment.
- *50proteins*: This dataset is about drug-protein binding prediction. Again, drugs are treated as input graphs while proteins are labels. We obtain the raw version from BindingDB<sup>2</sup>. In this dataset, the number of unique proteins (also called targets) is 595 and the number of unique drugs (or ligands) is 55,781. We select top 50 proteins that are bound by most ligands to construct our experimental dataset. There are 36,349 ligands in total with the average number of proteins that one ligand binds to is 1.35.

We divide each dataset into train/valid/test sets with the proportions of 0.6/0.2/0.2, respectively. The detailed statistics are shown in Table. 2 and the number of label occurrences is shown in Fig. 2. It is clear that the labels in *50proteins* are sparse as each ligand links to at most 10 proteins (and usually 1 or 2). Meanwhile, the labels in *9cancers* are denser with nearly a thousand of drugs positive to all cancers.

#### 4.1.2 Baselines

For comparison, we employ the following data representations and associated multilabel classifiers:

<sup>1</sup> <https://pubchem.ncbi.nlm.nih.gov/>

<sup>2</sup> <http://www.bindingdb.org/bind/index.jsp>

Assay ID	Cancer Type	%Positive
1	Lung	12.28
33	Melanoma	9.97
41	Prostate	11.77
47	Central Nervous System	12.22
81	Colon	14.50
83	Breast	16.22
109	Ovarian	12.76
123	Leukemia	18.91
145	Renal	12.03

Table 1: Assay ID and name of nine cancers in *9cancers* dataset. %Positive denotes the average percentage of positive examples for each cancer type over the total number of 13,356 molecules.

Dataset	#labels	avg. #nodes	avg. #edges	#node types	#edge types
9cancers	9	27.68	29.95	43	4
50proteins	50	25.31	27.49	14	4

Table 2: Statistics of all multilabel datasets with graph-structured inputs.

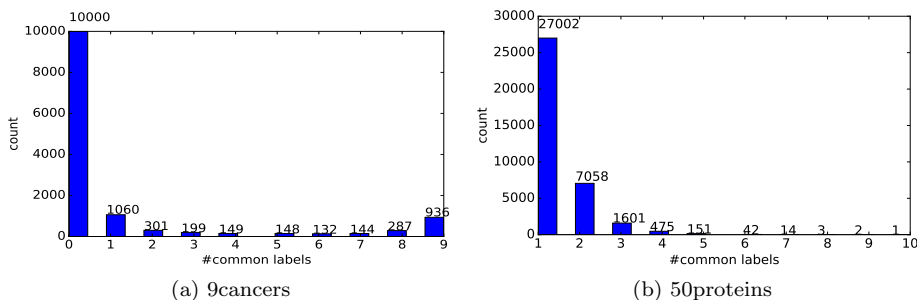


Fig. 2: Histogram of the number of common labels that each instance associates to in *9cancers* and *50proteins*

*Molecular fingerprint.* The first representation of molecules is a classical method known as molecular fingerprint—a set of substructure descriptors extracted from molecular graphs. Specifically, we use the well-known Morgan algorithm from RDKit<sup>3</sup> to generate multiple fingerprints with increasing radius from 1 to 5 to account for fine-grained levels of substructures. Then, these fingerprints are concatenated to form a final feature vector. For each radius, we set the length of the fingerprint hash vector to 100. This results in the final feature vector of size 500. We use two classifiers to run on top of this vector representation:

- The first is an SVM with RBF kernels which set as a base classifier for Binary Relevance algorithm [43]. We denote this model as fp+SVM.

<sup>3</sup> <http://www.rdkit.org/>

- The second classifier is a Highway Network (HWN) – a powerful deep neural network that maps an input vector to an output vector [38]. The dependencies among labels are implicitly captured through the intermediate hidden layers. We denote the combination of fingerprint and HWN as fp+HWN.

*String representation.* String is a machine readable format of molecule. We use SMILES<sup>4</sup> to represent molecules as strings. These strings are input to GRU, a recurrent network which works well on strings [7]. When reaching the end of the sequences, the last state of the recurrent network is fed to a 2-layer MLP that outputs prediction for all labels. This SMILES+GRU combination has been recently proven to be highly effective in drug evaluation and design [36].

*Graph representation.* The last set of baselines handle graph-structured input directly. We select two representative models: Weisfeiler-Lehman Graph Kernels (WL) [37] for graph kernel based methods and Column Networks (CLN) [30] for graph neural network based methods.

- For WL, we precompute the kernel matrix for both training and testing data using WL algorithm. The height of the rooted tree is chosen to be three. For *9cancers*, it results in about 49 thousand different tree structures for all nodes in the graph dataset. Meanwhile, the total number of graphs is only about 13 thousands. Therefore, increasing height more than three will add very little information about graph similarity as the number of matching substructures approach zero. The kernel matrix for training graphs is used as input to an SVM wrapped by Binary Relevance (WL+BR).
- For CLN, we use the same model as in [30] with a mean pooling layer on top message passing layers to compute the graph representation vector. This vector is then fed to a 2-layer MLP to predict all labels. CLN differs from our model mainly in the way of label estimation. That is, CLN delays the estimation of label until estimation of graph representation has finished. On the contrary, our method estimate the labels in parallel and in conjunction with graph embedding through message passing between graph and labels.

The hyper-parameters of fp+HWN and SMILES+GRU are obtained through validation. Meanwhile, the hyper-parameters of CLN are set similar to the optimal hyper-parameters of our model (see below).

#### 4.1.3 Model setting

In our model, the size of node and edge embedding is set to 50. We perform grid search for other hyper-parameters with the label embedding size in {10, 30, 50, 70, 100}, the number of factors in {1, 5, 10, 15, 20}, and the number of message passing layers in {2, 4, 6, 8, 10}. Dropout is set for every graph input node with the rate of 0.3. We do not use dropout for label nodes as it results

---

<sup>4</sup> [https://en.wikipedia.org/wiki/Simplified\\_molecular-input\\_line-entry\\_system](https://en.wikipedia.org/wiki/Simplified_molecular-input_line-entry_system)

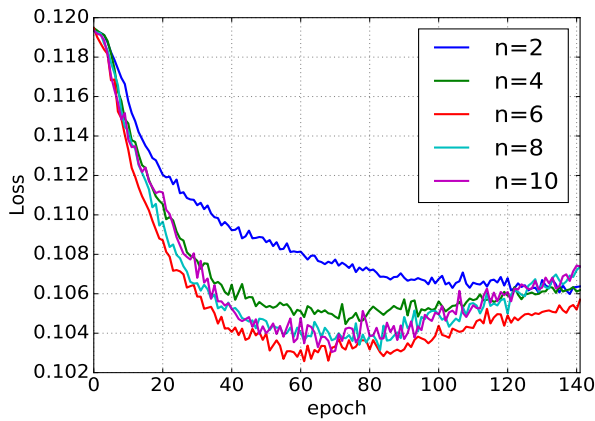


Fig. 3: Learning curves on *50proteins* with different number of message passing layers  $n \in \{2, 4, 6, 8, 10\}$ . Best viewed in color.

in low F1 score although it makes model less overfitting. In addition, we set the batch size to 60 and 100 for *9cancers* and *50proteins*, respectively. We use Adam [20] as an optimizer with an initial learning rate of 0.001. During training, the learning rate will be reduced by half if the validation loss does not improve after 20 consecutive epochs. We train our model for a maximum of 300 epochs and may stop early after decaying the learning rate 4 times.

#### 4.1.4 Evaluation metrics

We use popular metrics for multilabel classification which are micro, macro (sometimes called per label) F1 and micro, macro AUC. While micro F1 favors labels with many examples due to its global averaging, macro F1 treats all labels equally regardless of their sample size, hence, is a good indication of the model performance on small labels.

#### 4.1.5 Parameter sensitivity

To have a deep understanding of how GAML works for graph structured input, we investigate the contribution of different hyper-parameters including: the number of message passing layers (Fig. 3 and Fig. 4), the number of attention factors (Fig. 6), and the type of attention (Fig. 5). We report results for *50proteins*, but similar results are also observed for *9cancers*.

From Fig. 4, it is seen that when the number of layers  $n$  is small, e.g.  $n=2$ , the model performs very poorly. Increasing the number of layers usually improves the results. It is because at higher level, input nodes receive more structure information through message passing. However, when  $n \geq 6$ , the improvement rate becomes steady and the model is more likely to overfit (see Fig. 4c). We

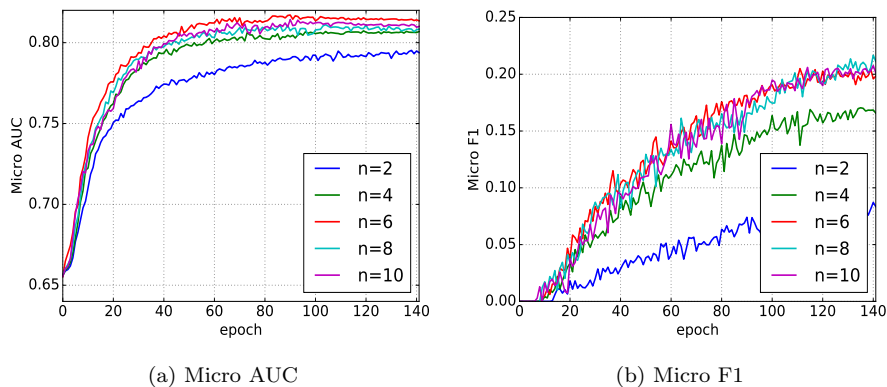


Fig. 4: Micro AUC (a) and Micro F1 (b) on 50proteins with different number of message passing layers  $n \in \{2, 4, 6, 8, 10\}$ . Best viewed in color.

think there are two reasons for this situation: (i) the structure information from distant nodes is much less important than from close neighbors; and (ii) the structure information at every node becomes more global and indistinguishable, causing difficulty for the model to detect meaningful substructures during prediction.

Another factor that affects the model performance is the type of attention. Generally, using attention provides better F1 score than not using it. However, label-to-input attention seems to be redundant and causes misleading to the model. We observed that when input-to-label attention is available, the model always has higher loss and lower AUC (see Fig. 5a and c). Meanwhile, label-to-input attention is important as it helps label nodes focus on particular substructures of the input graph to give accurate prediction. One interesting thing to note here is that the improvement of F1 mainly comes from Recall (as can be seen from Fig. 5b, d, e) and since the denominator in the Recall formula is constant (which is equal to the number of positive examples in the dataset), the number of true positives actually increases by attention.

GAML performs worst in term of both AUC and F1 when the number of attention factors  $k$  is 1 since there is no attention in this case. For other values from 10 to 20, the results are quite comparable, which suggests that a small value of  $k$  is usually sufficient.

#### 4.1.6 Performance results

Table 3 shows the classification results for graph structured input. Our model consistently beat all baselines on all evaluation metrics. In particular, our model achieves about 2%-3% higher F1 and about 0.25%-1% higher AUC than the second best method (CLN) on both datasets. We believe this improvement comes from the fact that our model can associate labels with useful substructure-

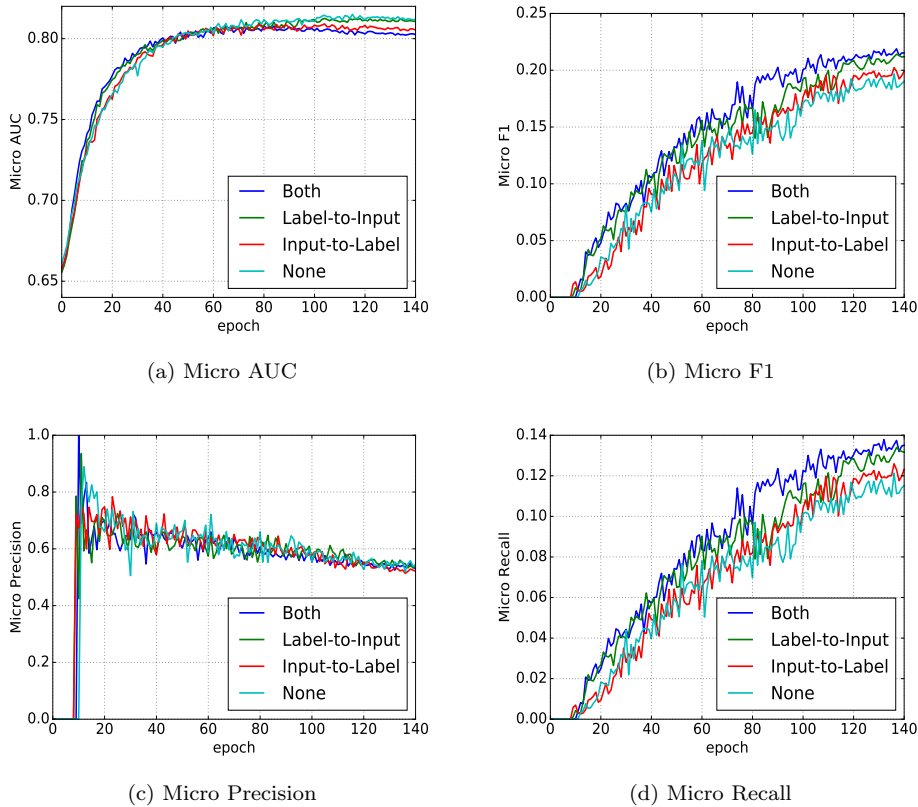


Fig. 5: Results on *50proteins* with different type of attentions. *Label-to-Input* refers to unidirectional attention from label to input nodes; *Input-to-Label* refers to attention in the reverse direction; *Both* refers to bidirectional attention. Best viewed in color.

tures from the input graph through attention mechanism while CLN does not have this capability. Furthermore, it is also clear that the models learning directly on graphs such as WL+BR or CLN usually provide better results than those learning on strings or vectors. For example, CLN achieves roughly 2% improvement in term of micro and macro F1 compared to its vector counterpart fp+HWN. Whereas, WL+BR produces about 2-4% higher macro and micro AUC than fp+SVM+BR.

#### 4.1.7 External knowledge of label dependencies

*A priori* label dependencies are known to improve model performance as they bring structure and constraints into the output space [23, 42]. We consider the setting where dependencies form a label graph. The multilabeling becomes



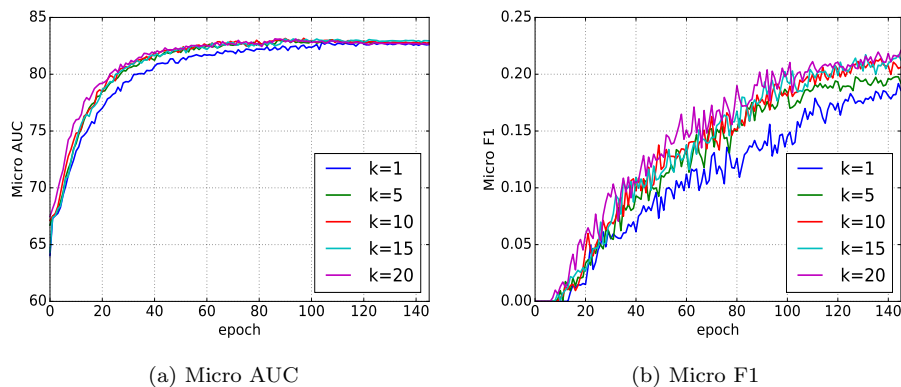


Fig. 6: Micro AUC (a) and Micro F1 (b) on 50proteins with different number of factors  $k \in \{1, 5, 10, 15, 20\}$ . Best viewed in color.

Dataset	Metrics	SVM	HWN	GRU	WL+BR	CLN	GAML
9 cancers	m-AUC	81.94	85.95	83.29	86.06	88.35	<b>88.78</b>
	M-AUC	81.37	85.85	82.74	85.74	88.23	<b>88.50</b>
	m-F1	50.63	57.44	55.97	54.55	59.48	<b>62.03</b>
	M-F1	50.71	57.29	55.99	54.54	59.50	<b>62.14</b>
50 proteins	m-AUC	79.85	77.46	79.11	81.62	82.08	<b>82.82</b>
	M-AUC	74.77	73.78	75.25	77.60	78.36	<b>79.35</b>
	m-F1	17.21	16.37	16.08	17.04	18.37	<b>20.47</b>
	M-F1	18.40	15.87	14.96	18.66	17.72	<b>19.83</b>

Table 3: The performance in the multi-label classification with graph-structured input (m-X: micro average of X; M-X: macro average). SVM and HWN work on fingerprint representation; GRU works on string representation of molecule known as SMILES; WL+BR and CLN work directly on graph representation. Bold indicates better accuracy.

node classification in the label graph *conditioned on the input graph*. We investigate the case of *50proteins* where the labels are sparse. The degree of protein-protein interactions (PPIs) was retrieved from Human Integrated Protein-Protein Interaction rEference (HIPPIE) [1]. HIPPIE scores are derived from other major PPI sources, reflecting the number of studies and the number of non-human organisms in which a PPI was found, as well as the quality of the techniques detecting the interaction. The PPI scores are normalized in the range of  $[0, 1]$ . Then we add an edge between two proteins if their interaction score is larger than a predefined threshold (which set to 0.5 in our experiment). Since the interaction scores are asymmetric, the edges are directed. Table 4 reports results of our model when external label dependencies are introduced. The results are improved on F1 measures but not on the AUC scores suggesting

Model	<i>50proteins</i>			
	m-AUC	M-AUC	m-F1	M-F1
GAML	<b>82.82</b>	<b>79.35</b>	20.47	19.83
GAML + PPI	82.61	79.29	<b>21.15</b>	<b>20.28</b>

Table 4: Results on incorporating external knowledge of label dependencies. Bold indicates better accuracy.

that the external label constraints may help balance recall and precision when labels are sparse.

#### 4.1.8 Attention visualization

In Fig. 7, we show the label-to-input attention scores at different layers when our model runs on *9cancers* to see how our model matches between labels and substructures of the input graph. We see that at the first layer, the label nodes often attend to many input nodes. The reason is that input nodes at this level only contain information about their types. In addition, the attended input nodes are usually special atoms like Oxygen (8) or Nitrogen (7) instead of the common Carbon (6). However, the attention becomes more focused when going up to higher layer since the structure information at each input node has been updated via message passing. Sometimes, new substructures emerge and the model may switch its attention to these substructures if it finds them to be more appropriate.

From the label-to-input attention matrices in Fig. 7, we can map back to the molecule graph to detect meaningful substructures toward labels. As shown in Fig. 8, we can observe the shift in the model attention with respect to the evolution of structures across layers. In particular, at layer 2, the model focuses most on the O-N substructure. However, at layer 3, the model changes its attention to N[6], N[5] and C[11] instead of Os. The reason is that the model becomes more interested in the appearance of two adjacent Ns in an aromatic group, which cannot be captured within two hops by starting at O. Therefore, an *attention shift* is performed by the model.

Note that although the attention shift looks disruptive in Fig. 7 as the model is highly attentive (due to well training), it is actually smooth under graphical view in Fig. 8 since the substructures rooted at N[6], N[5] and C[11] all contains the substructure O-N from the previous layer. This suggests a human-like concept transferring mechanism through attention where the old concept is not totally discarded but still exists as part of the new concept with less focusing from the brain. From layer 3 to layer 6, the model performs one more small attention shift (from N[6] to N[8]). We think the model does that to keep itself attended to the left ring only (instead of both the left and the right rings). This is reasonable because when N[8] receives more redundant information about the right ring, its attention score reduces from 0.48 (the 5-th row) to 0.27 (the 6-th row). The strong focus of the model on a particular substructure is also well demonstrated in Fig. 8. As we can see in the last

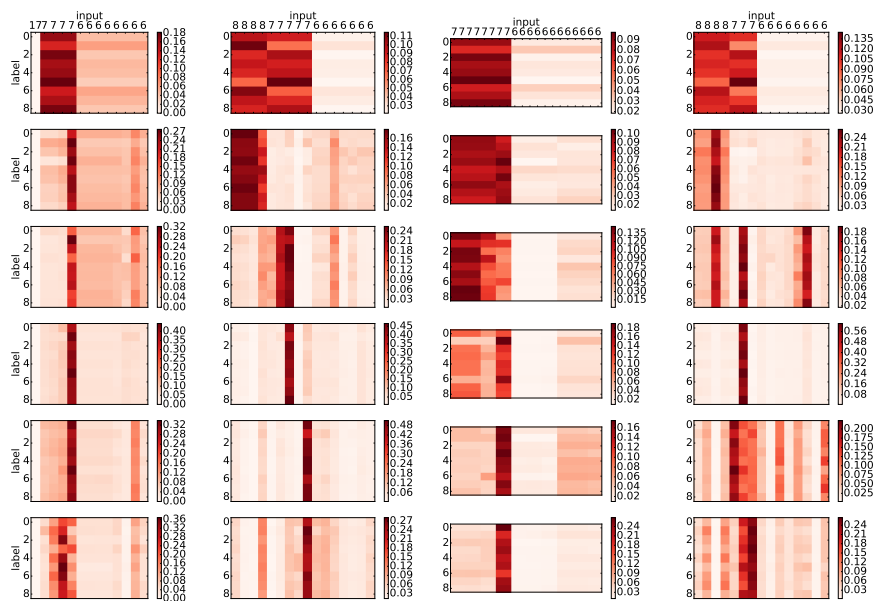


Fig. 7: Normalized label-to-input attention probability at 6 layers of GAML over 4 different molecular graphs sampled from *9cancers*. Darker color refers to higher probability. Columns correspond to input graphs and rows correspond to layers with the first layer drawn on top then the second layer and so on. Each tick in the x-axis is labeled with the atomic number of the corresponding node in the input graph (6: Carbon, 7: Nitrogen, 8: Oxygen, 17: Chlorine).

row, although C[10] (at the last column) contains information about the whole molecular graph, its attention score is still significantly smaller than of the substructure rooted at N[8].

#### 4.2 Multilabel classification with unstructured input

We now test whether the message passing scheme introduced in this paper can work on the traditional setting where the input is vector.

##### 4.2.1 Datasets

Four datasets were used in the experiments: *media\_mill*, *bookmarks*, *Corel5k* and *NUS-WIDE* (see Table 5 for statistics). The former two belong to the text categorization domain where each instance is a document represented as binary bag-of-words. Meanwhile, the latter two are for image classification problems where each image is represented as a real-value feature vector. For all datasets, we follow the predefined train/test split so that our results can be comparable to other methods.

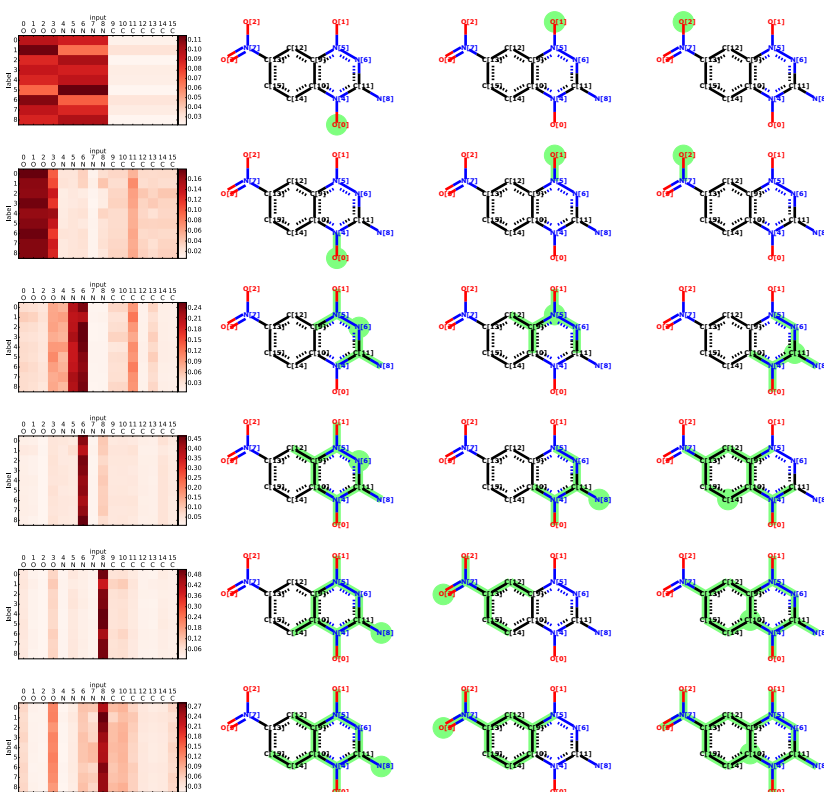


Fig. 8: Attention visualization on substructures of a molecule with PubChem SID of 491286. This molecule is the second example in Fig. 7. Each row specifies the top 3 substructures with the highest attention score (sorted in descending order from left to right) at the corresponding layer. For each substructure at layer  $k$ , the root atom as well as its neighbor atoms and bonds up to  $k$  hops are highlighted in green. Each atom is displayed with its atomic number and its index number (in square brackets) in the molecule.

Dataset	#labels	#features	#total	#train	#test
<i>media_mill</i>	101	120	43,907	30,993	12,914
<i>bookmarks</i>	208	2150	87,856	70,285	17,571
<i>Corel5k</i>	374	499	5,000	4,500	500
<i>NUS-WIDE</i>	81	128	269,648	161,789	107,859

Table 5: Statistics of all multilabel datasets with unstructured input.

### 4.2.2 Baselines

For comparison, we consider the following methods:

- State-of-the-art classical methods for multilabel classification (MLC) evaluated in [26], which are representative for broader classes of algorithms. For example, RAKEL [46] for ensemble methods, ML-kNN [51] for algorithm adaptation methods, HOMER [44] for label power set methods and Calibrated Label Ranking [12] for pairwise ranking. Most of these methods are implemented in popular multilabel machine learning systems, such as Mulan [45] or Meka [33]. Furthermore, for each combination of method and dataset, the authors performed cross-validation to search for optimal parameters.
- Collective multilabel classification with CRF (CML) [13]. This model can learn pairwise correlations among labels via CRF, hence, should be selected as baseline for comparison. We use the Java implementation of CML released on Github<sup>5</sup> and search for the optimal values of “train.gaussianVariance” in {0.01, 0.03, 0.1, 0.3, 1, 3, 10}. However, we can only test this model on *media\_mill* and *NUS-WIDE* since the other two datasets are not accepted by the implementation.
- A Highway Network (HWN) [38], similar to what used in Section 4.1. HWN shares the skip-connection structure implemented in our model. Hence the main difference between HWN and ours is the method of label estimation. In HWN, label estimation is delayed until features have been estimated. In our method, label estimation is performed simultaneously with feature estimation. Second, by using more than one factor, a richer set of feature aspects is extracted and distributed to labels in our method. To tune the HWN for the best performance, we conduct grid search on various pairs of the number of layers and the hidden size.

### 4.2.3 Model setting

The label embedding size is set to 50 for *NUS-WIDE* and *media\_mill*, 75 for *bookmarks* and 30 for *Corel5k*. We project input vector to a low dimensional space by using a single layer neural network with ReLU activation before feeding it to GAML. The size of the projected vector is 55 for *NUS-WIDE*, 75 for *media\_mill*, 110 for *bookmarks* and 50 for *Corel5k*. For all datasets, the number of message passing layers is set to 6. In training, the batch size for *NUS-WIDE* is 500 while for the other datasets, it is 100. We use  $k$ -fold cross validation where  $k$  is 9 for *Corel5k* and 5 for other dataset. The optimizer is Adam with an initial learning rate of 0.001. We reduce the learning rate by half if the valid loss does not decrease after 5 consecutive epochs for *Corel5k* and 20 for other datasets. The maximum number of epochs is 300 and the early stopping condition is 4 times of the learning rate decay.

<sup>5</sup> <https://github.com/cheng-li/pyramid/wiki/CRF>

Dataset	Metrics	Best in [26]	CML [13]	HWN	GAML
media.mill	m-F1	56.3	45.78	56.73	<b>57.53</b>
	M-F1	11.3	3.95	13.50	<b>14.17</b>
bookmarks	m-F1	26.8	-	32.51	<b>33.33</b>
	M-F1	11.9	-	20.43	<b>21.68</b>
Corel5k	m-F1	<b>29.3</b>	-	15.28	22.13
	M-F1	<b>4.2</b>	-	1.83	3.82
NUS-WIDE	m-F1	-	30.42	38.50	<b>39.83</b>
	M-F1	-	3.84	9.31	<b>11.38</b>

Table 6: The performance in the multi-label classification with unstructured input (m-X: micro average of X, M-X: macro average of X). Bold indicates better accuracy.

#### 4.2.4 Results

The classification performance of all the methods is presented in Table 6. The deep networks, HWN and GAML, outperform traditional methods and CML on most datasets except for *Corel5k*, which is the smallest dataset. Especially, on *bookmarks*, our model improves the micro F1 and macro F1 over the best traditional methods by about 7% and 10%, respectively. In the case of *Corel5k*, the best traditional method is CLR (see [26]), a ranking-based method that uses SVM as a base classifier. SVM appears to be more robust than deep networks on small datasets like *Corel5k*. Compared to HWN, GAML achieves better results on all datasets. This supports our model’s strength in learning correlations between labels and the input at multiple levels of abstraction.

## 5 Discussion

We introduced GAML, a new graph neural network to tackle an open problem of multi-label learning over graph-structured data. The key insight is to realize that label nodes and input nodes can be put into a joint graph to model the multi-way relationships among labels and subgraphs. This is achieved through a message passing scheme that exchanges information between connected nodes at multiple step and an attention mechanism that enables selective flowing of information between label nodes and input nodes. Our model design is highly flexible and scalable. We evaluated GAML using an extensive set of experiments on drug multi-targeting (protein binding and cancer response), as well as on datasets with unstructured inputs. Our results clearly demonstrate the efficacy of the proposed model.

This work opens up a wide room for the future at both applied and theoretical fronts. GAML is directly applicable to many other domains. One example is shopping basket recommendation, where users play the role of labels (with or without profile), and item basket modeled as input graph of items. Alternatively, items recommendation to user group works in a similar way, where the user group forms a social graph, and items play the role of

labels. At the modeling front, a next step is to extend GAML from label node classification to full graph prediction, where edges are also predicted. Additionally, the current setting is open for auxiliary tasks, e.g., the input graph is node-labeled.

## References

1. Gregorio Alanis-Lobato, Miguel A Andrade-Navarro, and Martin H Schaefer. HIPPIE v2. 0: enhancing meaningfulness and reliability of protein-protein interaction networks. *Nucleic Acids Research*, page gkw985, 2016.
2. Dzmitry Bahdanau, Kyunghyun Cho, and Yoshua Bengio. Neural machine translation by jointly learning to align and translate. *arXiv preprint arXiv:1409.0473*, 2014.
3. Wei Bi and James T Kwok. Multi-label classification on tree-and dag-structured hierarchies. In *Proceedings of the 28th International Conference on Machine Learning (ICML-11)*, pages 17–24, 2011.
4. Joan Bruna, Wojciech Zaremba, Arthur Szlam, and Yann LeCun. Spectral networks and locally connected networks on graphs. *arXiv preprint arXiv:1312.6203*, 2013.
5. Meihao Chen, Zhuoru Lin, and Kyunghyun Cho. Graph convolutional networks for classification with a structured label space. *arXiv preprint arXiv:1710.04908*, 2018.
6. Shang-Fu Chen, Yi-Chen Chen, Chih-Kuan Yeh, and Yu-Chiang Frank Wang. Order-free rnn with visual attention for multi-label classification. *arXiv preprint arXiv:1707.05495*, 2017.
7. Kyunghyun Cho, Bart Van Merriënboer, Caglar Gulcehre, Dzmitry Bahdanau, Fethi Bougares, Holger Schwenk, and Yoshua Bengio. Learning phrase representations using rnn encoder-decoder for statistical machine translation. *arXiv preprint arXiv:1406.1078*, 2014.
8. Michaël Defferrard, Xavier Bresson, and Pierre Vandergheynst. Convolutional neural networks on graphs with fast localized spectral filtering. In *Advances in Neural Information Processing Systems*, pages 3844–3852, 2016.
9. Krzysztof Dembczynski, Weiwei Cheng, and Eyke Hüllermeier. Bayes optimal multilabel classification via probabilistic classifier chains. In *ICML*, volume 10, pages 279–286, 2010.
10. Jia Deng, Nan Ding, Yangqing Jia, Andrea Frome, Kevin Murphy, Samy Bengio, Yuan Li, Hartmut Neven, and Hartwig Adam. Large-scale object classification using label relation graphs. In *European conference on computer vision*, pages 48–64. Springer, 2014.
11. Alex Fout, Jonathon Byrd, Basir Shariat, and Asa Ben-Hur. Protein interface prediction using graph convolutional networks. In *Advances in Neural Information Processing Systems*, pages 6533–6542, 2017.
12. Johannes Fürnkranz, Eyke Hüllermeier, Eneldo Loza Mencía, and Klaus Brinker. Multilabel classification via calibrated label ranking. *Machine learning*, 73(2):133–153, 2008.
13. N. Ghamrawi and A. McCallum. Collective multi-label classification. In *Proceedings of the 14th ACM international conference on Information and knowledge management*, pages 195–200. ACM New York, NY, USA, 2005.
14. Justin Gilmer, Samuel S Schoenholz, Patrick F Riley, Oriol Vinyals, and George E Dahl. Neural message passing for quantum chemistry. *ICML*, 2017.
15. Yunchao Gong, Yangqing Jia, Thomas Leung, Alexander Toshev, and Sergey Ioffe. Deep convolutional ranking for multilabel image annotation. *arXiv preprint arXiv:1312.4894*, 2013.
16. Aditya Grover and Jure Leskovec. node2vec: Scalable feature learning for networks. In *Proceedings of the 22nd ACM SIGKDD international conference on Knowledge discovery and data mining*, pages 855–864. ACM, 2016.
17. Yuhong Guo and Suicheng Gu. Multi-label classification using conditional dependency networks. In *IJCAI Proceedings-International Joint Conference on Artificial Intelligence*, volume 22, page 1300, 2011.

18. Will Hamilton, Zhitao Ying, and Jure Leskovec. Inductive representation learning on large graphs. In *Advances in Neural Information Processing Systems*, pages 1025–1035, 2017.
19. Wengong Jin, Regina Barzilay, and Tommi Jaakkola. Junction tree variational autoencoder for molecular graph generation. *arXiv preprint arXiv:1802.04364*, 2018.
20. Diederik Kingma and Jimmy Ba. Adam: A method for stochastic optimization. *arXiv preprint arXiv:1412.6980*, 2014.
21. Thomas N Kipf and Max Welling. Semi-supervised classification with graph convolutional networks. *arXiv preprint arXiv:1609.02907*, 2016.
22. Xiangnan Kong and S Yu Philip. gmlc: a multi-label feature selection framework for graph classification. *Knowledge and Information Systems*, 31(2):281–305, 2012.
23. J. Lafferty, A. McCallum, and F. Pereira. Conditional random fields: Probabilistic models for segmenting and labeling sequence data. In *Proceedings of the International Conference on Machine Learning (ICML)*, pages 282–289, 2001.
24. Sheng Li, Ming Shao, and Yun Fu. Multi-view low-rank analysis for outlier detection. In *Proceedings of the 2015 SIAM International Conference on Data Mining*, pages 748–756. SIAM, 2015.
25. Yujia Li, Daniel Tarlow, Marc Brockschmidt, and Richard Zemel. Gated graph sequence neural networks. *ICLR*, 2016.
26. Gjorgji Madjarov, Dragi Kocev, Dejan Gjorgjevikj, and Sašo Džeroski. An extensive experimental comparison of methods for multi-label learning. *Pattern recognition*, 45(9):3084–3104, 2012.
27. Asher Mullard. New drugs cost US [dollar] 2.6 billion to develop. *Nature Reviews Drug Discovery*, 13(12):877–877, 2014.
28. Mathias Niepert, Mohamed Ahmed, and Konstantin Kutikov. Learning convolutional neural networks for graphs. In *Proceedings of the 33rd annual international conference on machine learning. ACM*, 2016.
29. Bryan Perozzi, Rami Al-Rfou, and Steven Skiena. Deepwalk: Online learning of social representations. In *Proceedings of the 20th ACM SIGKDD international conference on Knowledge discovery and data mining*, pages 701–710. ACM, 2014.
30. Trang Pham, Truyen Tran, Dinh Phung, and Svetha Venkatesh. Column networks for collective classification. *AAAI*, 2017.
31. Trang Pham, Truyen Tran, and Svetha Venkatesh. One size fits many: Column bundle for multi-x learning. *arXiv preprint arXiv:1702.07021*, 2017.
32. Trang Pham, Truyen Tran, and Svetha Venkatesh. Graph memory networks for molecular activity prediction. *arXiv preprint arXiv:1801.02622*, 2018.
33. Jesse Read, Peter Reutemann, Bernhard Pfahringer, and Geoff Holmes. Meka: a multi-label/multi-target extension to weka. *The Journal of Machine Learning Research*, 17(1):667–671, 2016.
34. Franco Scarselli, Marco Gori, Ah Chung Tsoi, Markus Hagenbuchner, and Gabriele Monfardini. The graph neural network model. *IEEE Transactions on Neural Networks*, 20(1):61–80, 2009.
35. Michael Schlichtkrull, Thomas N Kipf, Peter Bloem, Rianne van den Berg, Ivan Titov, and Max Welling. Modeling relational data with graph convolutional networks. *arXiv preprint arXiv:1703.06103*, 2017.
36. Marwin HS Segler, Thierry Kogej, Christian Tyrchan, and Mark P Waller. Generating focused molecule libraries for drug discovery with recurrent neural networks. *ACS Central Science*, 2017.
37. Nino Shervashidze, Pascal Schweitzer, Erik Jan van Leeuwen, Kurt Mehlhorn, and Karsten M Borgwardt. Weisfeiler-lehman graph kernels. *Journal of Machine Learning Research*, 12(Sep):2539–2561, 2011.
38. Rupesh K Srivastava, Klaus Greff, and Jürgen Schmidhuber. Training very deep networks. In *Advances in neural information processing systems*, pages 2377–2385, 2015.
39. Liang Sun, Shuiwang Ji, and Jieping Ye. Canonical correlation analysis for multilabel classification: A least-squares formulation, extensions, and analysis. *IEEE Transactions on Pattern Analysis and Machine Intelligence*, 33(1):194–200, 2011.
40. Ichigaku Takigawa and Hiroshi Mamitsuka. Generalized sparse learning of linear models over the complete subgraph feature set. *IEEE transactions on pattern analysis and machine intelligence*, 39(3):617–624, 2017.



41. Damien Teney, Lingqiao Liu, and Anton van den Hengel. Graph-structured representations for visual question answering. *CVPR*, 2017.
42. I. Tsochantaridis, T. Hofmann, T. Joachims, and Y. Altun. Support vector machine learning for interdependent and structured output spaces. In *Proceedings of the International Conference on Machine Learning (ICML)*, pages 823–830, 2004.
43. G. Tsoumakas and I. Katakis. Multi-label classification: An overview. *International Journal of Data Warehousing and Mining*, 3(3):1–13, 2007.
44. Grigorios Tsoumakas, Ioannis Katakis, and Ioannis Vlahavas. Effective and efficient multilabel classification in domains with large number of labels. In *Proc. ECML/PKDD 2008 Workshop on Mining Multidimensional Data (MMD'08)*, volume 21, pages 53–59. sn, 2008.
45. Grigorios Tsoumakas, Eleftherios Spyromitros-Xioufis, Jozef Vilcek, and Ioannis Vlahavas. Mulan: A java library for multi-label learning. *Journal of Machine Learning Research*, 12(Jul):2411–2414, 2011.
46. Grigorios Tsoumakas and Ioannis Vlahavas. Random k-labelsets: An ensemble method for multilabel classification. In *European conference on machine learning*, pages 406–417. Springer, 2007.
47. Jiang Wang, Yi Yang, Junhua Mao, Zhiheng Huang, Chang Huang, and Wei Xu. Cnn-rnn: A unified framework for multi-label image classification. In *Proceedings of the IEEE Conference on Computer Vision and Pattern Recognition*, pages 2285–2294, 2016.
48. Yunchao Wei, Wei Xia, Min Lin, Junshi Huang, Bingbing Ni, Jian Dong, Yao Zhao, and Shuicheng Yan. Hcp: A flexible cnn framework for multi-label image classification. *IEEE Transactions on Pattern Analysis and Machine Intelligence*, 38(9):1901–1907, 2016.
49. Kelvin Xu, Jimmy Ba, Ryan Kiros, Kyunghyun Cho, Aaron Courville, Ruslan Salakhudinov, Rich Zemel, and Yoshua Bengio. Show, attend and tell: Neural image caption generation with visual attention. In *International Conference on Machine Learning*, pages 2048–2057, 2015.
50. Chih-Kuan Yeh, Wei-Chieh Wu, Wei-Jen Ko, and Yu-Chiang Frank Wang. Learning deep latent space for multi-label classification. In *AAAI*, pages 2838–2844, 2017.
51. Min-Ling Zhang and Zhi-Hua Zhou. ML-KNN: A lazy learning approach to multi-label learning. *Pattern recognition*, 40(7):2038–2048, 2007.